Nanoscale Advances

COMMUNICATION

View Article Online
View Journal | View Issue

Cite this: *Nanoscale Adv.*, 2024, **6**, 5827

Received 13th August 2024
Accepted 31st October 2024

DOI: 10.1039/d4na00667d

rsc.li/nanoscale-advances

Porous pillar[6]arene-based polymers for reversible iodine capture†

Shujie Lin, Ziliang Zhang, Di Gao, Longming Chen, Chengyang Tian, Junyi Chen* and Qingbin Meng *

Iodine in nuclear waste can cause serious environment pollution and health risks, and has thus driven more development of materials for iodine capture. Herein, a novel porous pillar[6]arene-based polymer (P-P6APs) was easily prepared as a supramolecular adsorbent for iodine *via* a one-step crosslinking reaction between per-hydroxylated pillar[6]arene and decafluorobiphenyl. Nitrogen adsorption tests demonstrated that this material possessed a satisfactory surface area (S_{BET} = 366 m^2 g^{-1}) and pore diameter (3.8 nm), which was due to the macrocyclic scaffolds. Compared with commercially available activated carbon, P-P6APs exhibited superior adsorption efficiency toward volatile iodine not only in the solution phase (water and *n*-hexane) but also in the gas phase. This outcome was mainly ascribed to nonspecific adsorption by the pore structure of the crosslinked material coupled with multiple intermolecular binding sites of the macrocyclic scaffold. Moreover, this supramolecular absorbent was recyclable and could be reused 5 times with no obvious loss of performance.

Introduction

For the sustainable development of new energy sources, nuclear power is being used to solve the problem of energy shortages in more than thirty countries around the world.[1–4] However, a series of hazardous events, including the Chernobyl disaster and Fukushima accident occurred, producing a profound impact on surrounding areas.[5–8] The wastes involved (*e.g.* ^{129}I, ^{137}Cs, ^{90}Sr, ^{60}Co, *etc.*) are highly radioactive with extremely long half-lives, which evokes an essential question as to how to properly handle nuclear waste.[9–16] Iodine is a volatile product from uranium fission that is particularly problematic due to its solubility. Different isotopes of iodine present different issues for people and environment. ^{129}I has a half-life of 1.57 × 10^7 years and poses a long-term an environmental risk due to bioaccumulation,[17,18] while ^{131}I has a shorter half-life of 8.02 days and also poses serious harm to human health.[19–21] Exposure to these isotopes would induce leukopenia, hypothyroidism, cancer and so forth.[22–24] There is, therefore, an urgent need to develop efficient adsorbents to capture ionic and neutral iodine residues.

To date, many techniques have been developed to sequestrate iodine such as wet scrubbing,[25] mineral crystallisation,[26] glass sintering[27] and physical adsorption.[20] In particular, porous solid material-based adsorption methods show great potential for this specific task. Of these materials, the most representative types include polymers, organic cages, metal–organic frameworks, and covalent organic frameworks, although the uptake capacity and structural stability are hard to balance in many cases.[28–35] Macrocycles with distinctive pre-organized cavities and excellent recognition properties provide an alternative method for sequestering iodine.[36–39] Huang *et al.* reported that nonporous ethylated pillar[6]arene crystals, rather than the cyclic pentamer or heptamer, had the ability and the best performance for the capture of volatile iodine in the air or solution phase. The crystallography results proved that one molecule of pillar[6]arene could bind to an average of 2.2 iodine atoms, mainly driven by typical charge-transfer interactions.[40,41] Combined with the advantages of the above two types of material, we hypothesized that the introduction of a pillar[6]arene scaffold into a porous solid material would endow the resultant product with superior iodine adsorption potency.

In the present study, we have designed and prepared pillar[6]arene-based polymers (P-P6APs) *via* a one-step crosslinking reaction between a per-hydroxylated pillar[6]arene using known methods and commercially available decafluorobiphenyl (Scheme 1).[42,43] The inherent cyclic structure is a key factor to rendering P-P6APs porous. Compared to activated carbon with a similar surface area, this supramolecular absorbent exhibited superior adsorption efficiency toward volatile iodine, not only in

State Key Laboratory of National Security Specially Needed Medicines, Beijing Institute of Pharmacology and Toxicology, Beijing 100850, P. R. China. E-mail: jychen_msc@yeah.net; nankaimqb@sina.com

† Electronic supplementary information (ESI) available: General materials and methods, synthetic procedures, supporting results and experimental raw data. See DOI: https://doi.org/10.1039/d4na00667d

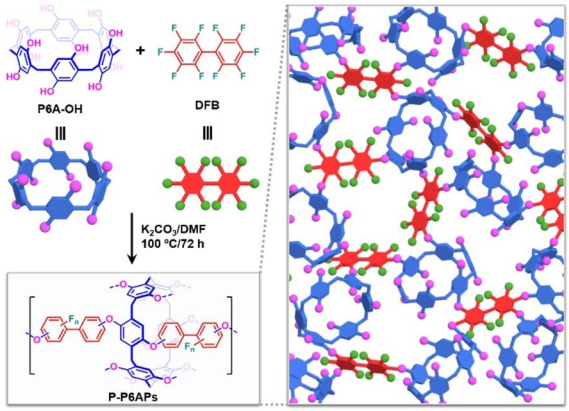

Scheme 1 Pillar[6]arene-based polymer networks derived from nucleophilic aromatic substitution reactions. Left: Synthesis of the high-surface-area porous P-P6APs from P6A-OH and DFB. Right: Schematic of the P-P6APs structure.

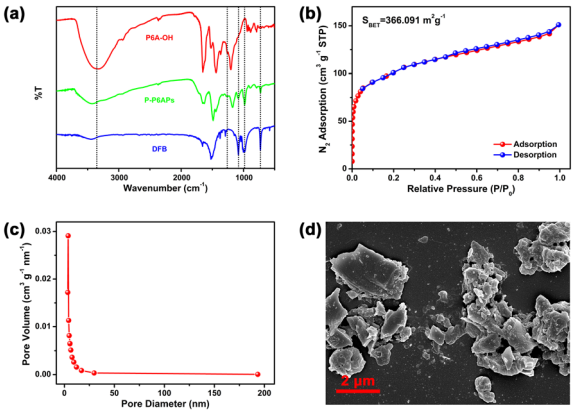

Fig. 1 (a) FT-IR spectra of P6A-OH, P-P6APs and DFB. (b) Nitrogen adsorption/desorption isotherm of P-P6APs. (c) The cumulative pore volume (pore diameter) of P-P6APs obtained *via* a Barrett–Joyner–Halenda analysis. (d) SEM image of P-P6APs.

the air, but also in an organic solvent and aqueous solution, due to nonspecific adsorption by the nanoscale pore structure coupled with multiple intermolecular interactions between the macrocyclic exterior and iodine molecule. The dynamic character of the noncovalent interactions and the insoluble nature of these crosslinked polymers facilitate the simple regeneration of P-P6APs, just by using washing and drying procedures.

Results and discussion

Firstly, per-hydroxylated pillar[6]arene (P6A-OH) was chosen as the macrocyclic precursor to prepare the porous polymers. As depicted in Scheme 1, P6A-OH was directly crosslinked with decafluorobiphenyl (DFB) in a suspension of K_2CO_3 in DMF at 100 °C. The crosslinking process involves a nucleophilic substitution reaction of the phenolic hydroxyl groups of P6A-OH to replace the fluoride on the DFB. After 72 h of heating, the prepared pillar[6]arene-based polymers (P-P6APs) precipitated out of the reaction liquid and then could be used following filtration, washing and drying. For comparison in the following experiments, monomer-containing polymers (MPs) were also constructed using the same method. Subsequently, Fourier-transform infrared (FT-IR) spectroscopy was employed to verify the molecular structure of P-P6APs. As shown in Fig. 1a, the C–F stretching bands of DFB at 1080 cm^{-1}, 981 cm^{-1} and 729 cm^{-1}, as well as the stretching vibrational absorption of the phenolic hydroxyl groups of P6A-OH at 3346 cm^{-1} could be found in FT-IR spectrum of P-P6APs. Meanwhile, new characteristic signals corresponding to the aromatic C-O-C stretching vibration appeared at 1230 cm^{-1}. These findings indicated that the desired product was successfully synthesized *via* the crosslinking reaction between P6A-OH and DFB. Additional FT-IR experiment also proved the formation of the MPs (Fig. S1†).

Next, nitrogen adsorption tests were performed to investigate the porosity of the prepared P-P6APs and MPs. A type IV isotherm with a visible hysteresis cycle could be observed within the relative pressure range of 0.5–1.0, and the Brunauer–Emmett–Teller (BET) specific surface area of P-P6APs was calculated to be 366 $m^2\ g^{-1}$, revealing that the crosslinked material has a relatively high porosity with mesopores in its interior (Fig. 1b). The corresponding pore size distribution curve of P-P6APs obtained from the nitrogen desorption data further demonstrated that the pore diameter was about 3.8 nm with a pore volume of 0.08 $cm^3\ g^{-1}$ (Fig. 1c). MPs, in contrast, exhibited almost no pore texture (Fig. S2 and S3†). These results led us to suggest that the macrocyclic scaffold building block was crucial for the porosity of P-P6APs. Moreover, the particles of P-P6APs exhibited a medium size of about 2 μm, as inferred from the scanning electron microscopic studies (Fig. 1d). The above surface area and aperture results led us to consider that P-P6APs could be an ideal candidate for absorbent materials.

As mentioned above, the pillar[6]arene skeleton has good ability to capture iodine molecules (I_2) *via* charge transfer. Hence we envisioned that the prepared absorbent P-P6APs could effectively capture I_2, in view of its porosity and exterior binding potency. First, the I_2 adsorption ability of P-P6APs was verified in I_2/KI solution, a typical source of I^-, I_2 and I_3^- based on dynamic equilibrium. As shown in Fig. 2a, 250 ppm of I_2/KI solution appeared brown and became almost colorless within 20 min after addition of P-P6APs. An appropriate curve was also derived to quantitatively assess the absorption efficiency of P-P6APs (Fig. S4†). The characteristic UV/vis peaks of the I_2/KI solution decreased in a time-dependent manner (Fig. 2b), and the uptake efficiency of P-P6APs could quickly reach 77.87% at 10 min after adding the absorbent (Fig. 2c). In addition, MPs and a commercially available activated carbon (AC) with a similar BET value to P-P6APs were chosen as negative and positive controls, respectively. Similar absorption could be observed in these two groups, while the uptake efficiencies were only 66.98% and 19.00% for AC and MPs, respectively (Fig. S5–S8†). These results demonstrated that the cyclic building blocks of P-P6APs were prerequisite to achieve its effective performance. Aside from the effectiveness, the selectivity is another requirement for an adsorbing material. To verify this,

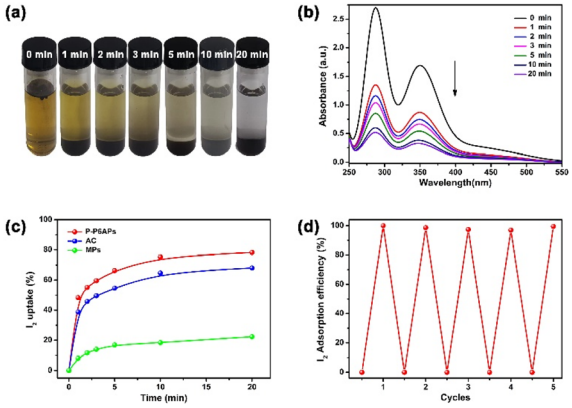

Fig. 2 (a) Photograph showing solution color change when 6.0 mg of P-P6APs was placed in I_2/KI (aq) (250 ppm). (b) Time-dependent UV/vis absorption spectra of I_2/KI (aq) (250 ppm) upon addition of P-P6APs (6.0 mg). (c) Time-dependent I_2 uptake efficiency based on the absorption peak at 286 nm after adding P-P6APs, AC and MPs. (d) Iodine adsorption efficiency of P-P6APs after the same material is recycled 5 times in I_2/KI (aq).

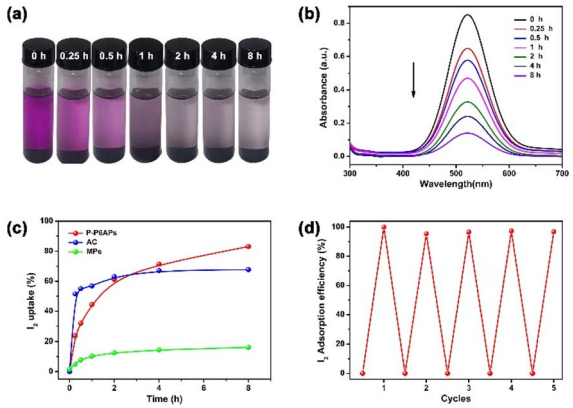

Fig. 3 (a) Photograph showing color change when 24.0 mg of P-P6APs was placed in an iodine/*n*-hexane solution (1 mM). (b) Time-dependent UV/vis absorption spectra of an iodine/*n*-hexane solution (1 mM) upon addition of P-P6APs (24.0 mg). (c) Time-dependent I_2 uptake efficiency based on the absorption peak at 520 nm after adding P-P6APs, AC and MPs. (d) Iodine adsorption efficiency of P-P6APs after the same material was recycled 5 times in an iodine/*n*-hexane solution.

adsorption experiments in a binary mixture consisting of a saturated iodine solution (250 ppm) and potassium salts of its competing anions (10 equivalents) were performed. As shown in Fig. S9,† the results proved that P-P6APs possessed specific adsorption selectivity for iodine. The effectiveness and selectivity of this supramolecular adsorbent were comparable to other typical adsorbents reported in the literature under conditions of capture from water (Table S1†). Furthermore, the ability to regenerate an adsorbent is another important factor affecting its practical application. When the absorption saturated P-P6APs was immersed in methanol, the I_2 was completely released. The resultant P-P6APs could be reused following a simple drying process and 99% of the initial adsorption efficiency was retained after five regeneration cycles (Fig. 2d).

Next, we utilized the I_2 removal application in organic systems as technical storage to counteract complex scenarios. As depicted in Fig. 3a, the purple I_2/*n*-hexane (1 mM) solution gradually faded and became colorless at about 8 h after addition of P-P6APs. A calibration curve was derived to calculate the I_2 concentration (Fig. S10†). Upon addition of P-P6APs to an I_2/*n*-hexane solution, the characteristic I_2 signal at 522 nm in *n*-hexane decreased from 0.85 to 0.14 over the duration of the test (Fig. 3b). The I_2 removal efficiency was calculated to be 83.51% at 8 h (Fig. 3c). The AC exhibited quicker absorption performance within the first 2 h, and the absorption amount soon reached saturation with a removal efficiency of 68.02% (Fig. S11 and S12†). For the MPs, the accumulative absorption amount was only 16.12% over the same measurement range (Fig. S13 and S14†). Similarly, we also confirmed that P-P6APs also could maintain its capture potency without decreasing I_2 uptake performance in *n*-hexane after being recycled five times (Fig. 3d).

Apart from applications in the solution phase highlighted above, we further wondered whether the supramolecular absorbent P-P6APs was able to uptake I_2 vapor. First, we exposed P-P6APs to I_2 vapor for 11 h. The color of the powder changed from black to brownish black (Fig. 4a and b), which could serve as preliminary evidence of successful adsorption. Furthermore, P-P6APs, AC and MPs were respectively placed in three pre-weighed vials, which were then enclosed in iodine-containing bottles and heated at 80 °C in an oven. By weighing at predetermined intervals, the time-dependent adsorption behaviors of three groups were examined and the results are presented in Fig. 4c. The I_2 vapor uptake of P-P6APs descended slowly as the adsorption time was extended and reached equilibrium at about 5 h with the uptake ratio found to be up to approximately 70 wt%. While under the same experimental conditions, the I_2 uptake ratios of AC and MPs were respectively only 24.79 wt% and 2.07 wt% within the same measurement range. Next, powder X-ray diffraction (PXRD) and FT-IR were performed to gain insight into the uptake process and the nature of the

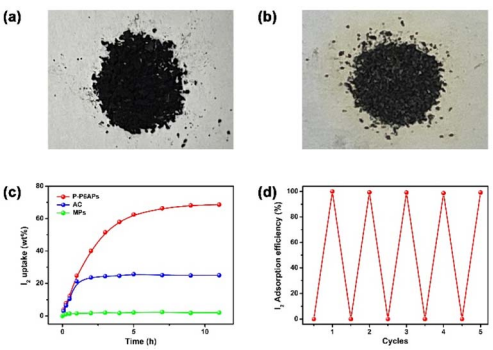

Fig. 4 Photos of P-P6APs (a) before and (b) after exposure to iodine vapor for 11 h. (c) Time-dependent I_2 vapor uptake efficiency of P-P6APs, AC and MPs at 80 °C. (d) Iodine adsorption efficiency of P-P6APs after the same material is recycled 5 times for iodine vapor capture.

adsorbed iodine. As shown in Fig. S15,† the PXRD measurements revealed that iodine was taken into the polymeric networks in a non-crystalline form. The adsorption of iodine caused the peaks in the FT-IR spectrum ascribed to the phenolic hydroxyl group at 3346 cm^{-1} to shift, and for the peaks of the phenyl rings at 1638, 1488 cm^{-1} and those of the C–F bond at 1080, 981 and 729 cm^{-1} to decrease in intensity (Fig. S16†). The results of the regeneration experiments proved that the I_2 vapor adsorption capacity of P-P6APs might not decline obviously after five cycles (Fig. 4d). Moreover, we have further investigated the adsorption performance after the sixth recycle of the material (Fig. S17†) and the adsorption efficiencies of P-P6APs could still reach 95% in three systems, revealing its good recyclability. On above basis, we have shown that macrocycle-based crosslinked material P-P6APs can be employed to effectively capture I_2 in both the solution phase (water and *n*-hexane) and vapor phase, and can be reused many times with no decrease in performance, mainly ascribed to non-covalent interactions. If these favorable results translate into practical use, P-P6APs is expected to provide a significant benefit for nuclear waste management.

Conclusion

In conclusion, we have successfully developed a pillar[6]arene-based crosslinked polymer as a supramolecular adsorbent for iodine capture. Nitrogen adsorption tests demonstrated that this material possessed satisfactory surface area and pore diameters, which was due to the macrocyclic scaffolds. Compared with two controls AC and MPs, P-P6APs could effectively capture I_2 in not only the solution phase (water and *n*-hexane), but also in the gas phase *via* intermolecular interactions. Its regeneration only requires washing and drying procedures, and it could be reused many times with no decrease in performance. This porous macrocycle-based material is poised for further development as a versatile tool for hazardous substance treatment.

Data availability

The authors confirm that the data supporting the findings of this study are available within the article and its ESI.†

Author contributions

Q. M., J. C. and S. L. conceived this project and designed the experiments. S. L. contributed to most of the experimental work. Z. Z., D. G., L. C. and C. T. carried out some of the experiments. Q. M., J. C. and S. L. analyzed the data. J. C. and S. L. co-wrote the paper. All authors discussed and commented on the paper.

Conflicts of interest

There are no conflicts to declare.

Acknowledgements

This research was financially supported by the National Natural Science Foundation of China (22171286, 22201212) and the China Postdoctoral Science Foundation (2023M734309).

Notes and references

1 L. Zhan, Y. Bo, T. Lin and Z. Fan, Development and outlook of advanced nuclear energy technology, *Energy Strategy Rev.*, 2021, **34**, 100630.
2 A. Adamantiades and I. Kessides, Nuclear power for sustainable development: Current status and future prospects, *Energy Policy*, 2009, **37**, 5149–5166.
3 M. Sadiq, R. Shinwari, M. Usman, I. Ozturk and A. I. Maghyereh, Linking nuclear energy, human development and carbon emission in BRICS region: Do external debt and financial globalization protect the environment?, *Nucl. Eng. Technol.*, 2022, **54**, 3299–3309.
4 Y. Wu, Y. Xie, X. Liu, Y. Li, J. Wang, Z. Chen, H. Yang, B. Hu, C. Shen, Z. Tang, Q. Huang and X. Wang, Functional nanomaterials for selective uranium recovery from seawater: Material design, extraction properties and mechanisms, *Coord. Chem. Rev.*, 2023, **483**, 215097.
5 G. Steinhauser, A. Brandl and T. E. Johnson, Comparison of the Chernobyl and Fukushima nuclear accidents: A review of the environmental impacts, *Sci. Total Environ.*, 2014, **470–471**, 800–817.
6 A. Aitsi-Selmi and V. Murray, The Chernobyl Disaster and Beyond: Implications of the Sendai Framework for Disaster Risk Reduction 2015-2030, *PLoS Med.*, 2016, **13**, e1002017.
7 A. R. Marks, The Fukushima nuclear disaster is ongoing, *J. Clin. Invest.*, 2016, **126**, 2385–2387.
8 T. Ohba, K. Tanigawa and L. Liutsko, Evacuation after a nuclear accident: Critical reviews of past nuclear accidents and proposal for future planning, *Environ. Int.*, 2021, **148**, 106379.
9 D. Alby, C. Charnay, M. Heran, B. Prelot and J. Zajac, Recent developments in nanostructured inorganic materials for sorption of cesium and strontium: Synthesis and shaping, sorption capacity, mechanisms, and selectivity-A review, *J. Hazard. Mater.*, 2018, **344**, 511–530.
10 D. Mei, L. Liu and B. Yan, Adsorption of uranium (VI) by metal-organic frameworks and covalent-organic frameworks from water, *Coord. Chem. Rev.*, 2023, **475**, 214917.
11 S. U. Nandanwar, K. Coldsnow, V. Utgikar, P. Sabharwall and D. E. Aston, Capture of harmful radioactive contaminants from off-gas stream using porous solid sorbents for clean environment-A review, *Chem. Eng. J.*, 2016, **306**, 369–381.
12 M. R. Awual, T. Yaitaa, T. Taguchi, H. Shiwakua, S. Suzuki and Y. Okamoto, Selective cesium removal from radioactive liquid waste by crown ether immobilized new class conjugate adsorbent, *J. Hazard. Mater.*, 2014, **278**, 227–235.
13 M. Rabiul Awual, S. Suzuki, T. Taguchi, H. Shiwaku, Y. Okamoto and T. Yaita, Radioactive cesium removal from

nuclear wastewater by novel inorganic and conjugate adsorbents, *Chem. Eng. J.*, 2014, **242**, 127–135.
14 D. Banerjee, C. M. Simon, A. M. Plonka, R. K. Motkuri, J. Liu, X. Chen, B. Smit, J. B. Parise, M. Haranczyk and P. K. Thallapally, Metal-organic framework with optimally selective xenon adsorption and separation, *Nat. Commun.*, 2016, **7**, 11831.
15 J. Li, X. Wang, G. Zhao, C. Chen, Z. Chai, A. Alsaedi, T. Hayat and X. Wang, Metal-organic framework-based materials: superior adsorbents for the capture of toxic and radioactive metal ions, *Chem. Soc. Rev.*, 2018, **47**, 2322–2356.
16 F.-F. Li, W.-R. Cui, W. Jiang, C.-R. Zhang, R.-P. Liang and J.-D. Qiu, Stable sp^2 carbon-conjugated covalent organic framework for detection and efficient adsorption of uranium from radioactive wastewater, *J. Hazard. Mater.*, 2020, **392**, 122333.
17 B. J. Riley, J. D. Vienna, D. M. Strachan, J. S. McCloy and J. L. Jerden Jr, Materials and processes for the effective capture and immobilization of radioiodine: A review, *J. Nucl. Mater.*, 2016, **470**, 307–326.
18 B. Li, B. Wang, X. Huang, L. Dai, L. Cui, J. Li, X. Jia and C. Li, Terphen[*n*]arenes and Quaterphen[*n*]arenes (n = 3–6): One-Pot Synthesis, Self-Assembly into Supramolecular Gels, and Iodine Capture, *Angew. Chem., Int. Ed.*, 2019, **58**, 3885–3889.
19 T. Pan, K. Yang, X. Dong and Y. Han, Adsorption-based capture of iodine and organic iodides: status and challenges, *J. Mater. Chem. A*, 2023, **11**, 5460–5475.
20 Y. Hao, Z. Tian, C. Liu and C. Xiao, Recent advances in the removal of radioactive iodine by bismuth-based materials, *Front. Chem.*, 2023, **11**, 1122484.
21 C. Muhire, A. T. Reda, D. Zhang, X. Xu and C. Cui, An overview on metal oxide-based materials for iodine capture and storage, *Chem. Eng. J.*, 2022, **431**, 133816.
22 K. Yamashita, S. Morimoto, S. Kimura, Y. Seki, K. Bokuda, D. Watanabe, T. Yazaki, K. Abe and A. Ichihara, Transient Leukopenia After Radioactive Iodine Treatment in Patients With Graves' Disease: A Retrospective Cohort Study, *J. Endocr. Soc.*, 2021, **5**, bvab039.
23 S. Leboulleux, I. Borget and M. Schlumberger, Post-operative radioactive iodine administration in patients with low-risk thyroid cancer, *Nat. Rev. Endocrinol.*, 2022, **18**, 585–586.
24 C. M. Kitahara, A. B. de Gonzalez, A. Bouville, A. B. Brill, M. M. Doody, D. R. Melo, S. L. Simon, J. A. Sosa, M. Tulchinsky, D. Villoing and D. L. Preston, Association of Radioactive Iodine Treatment With Cancer Mortality in Patients With Hyperthyroidism, *JAMA Intern. Med.*, 2019, **179**, 1034–1042.
25 C. D. O'Dowd, J. L. Jimenez, R. Bahreini, R. C. Flagan, J. H. Seinfeld, K. Hämerl, L. Pirjola, M. Kulmala and T. Hoffmann, Marine aerosol formation from biogenic iodine emissions, *Nature*, 2002, **417**, 632–636.
26 F. Audubert, J. Carpena, J. L. Lacout and F. Tetard, Elaboration of an iodine-bearing apatite Iodine diffusion into a $Pb_3(VO_4)_2$ matrix, *Solid State Ionics*, 1997, **95**, 113–119.
27 D. F. Sava, T. J. Garino and T. M. Nenoff, Iodine confinement into metal–organic frameworks (MOFs): low-temperature sintering glasses to form novel glass composite material (GCM) alternative waste forms, *Ind. Eng. Chem. Res.*, 2012, **51**, 614–620.
28 Y. Zhu, Y. Qi, X. Guo, M. Zhang, Z. Jia, C. Xia, N. Liu, C. Bai, L. Ma and Q. Wang, A crystalline covalent organic framework embedded with a crystalline supramolecular organic framework for efficient iodine capture, *J. Mater. Chem. A*, 2021, **9**, 16961–16966.
29 X. Zhang, J. Maddock, T. M. Nenoff, M. A. Denecke, S. Yang and M. Schröder, Adsorption of iodine in metal-organic framework materials, *Chem. Soc. Rev.*, 2022, **51**, 3243.
30 J. F. Kurisingal, H. Yun and C. S. Hong, Porous organic materials for iodine adsorption, *J. Hazard. Mater.*, 2023, **458**, 131835.
31 Y.-J. Liu, Y.-F. Sun1, S.-H. Shen, S.-T. Wang, Z.-H. Liu, W.-H. Fang, D. S. Wright and J. Zhang, Water-stable porous Al^{24} Archimedean solids for removal of trace iodine, *Nat. Commun.*, 2022, **13**, 6632.
32 Y. Xie, T. Pan, Q. Lei, C. Chen, X. Dong, Y. Yuan, J. Shen, Y. Cai, C. Zhou, I. Pinnau and Y. Han, Ionic Functionalization of Multivariate Covalent Organic Frameworks to Achieve an Exceptionally High Iodine-Capture Capacity, *Angew. Chem., Int. Ed.*, 2021, **60**, 22432–22440.
33 Y. Liao, J. Weber, B. M. Mills, Z. Ren and C. F. J. Faul, Highly Efficient and Reversible Iodine Capture in Hexaphenylbenzene-Based Conjugated Microporous Polymers, *Macromolecules*, 2016, **49**, 6322–6333.
34 W. Xie, D. Cui, S.-R. Zhang, Y.-H. Xu and D.-L. Jiang, Iodine capture in porous organic polymers and metal-organic frameworks materials, *Mater. Horiz.*, 2019, **6**, 1571–1595.
35 J. Huve, A. Ryzhikov, H. Nouali, V. Lalia, G. Augé and T. J. Daou, Porous sorbents for the capture of radioactive iodine compounds: a review, *RSC Adv.*, 2018, **8**, 29248–29273.
36 D. Li, G. Wu, Y.-K. Zhu and Y.-W. Yang, Phenyl-Extended Resorcin[4]arenes: Synthesis and Highly Efficient Iodine Adsorption, *Angew. Chem., Int. Ed.*, 2024, **10**, e202411261.
37 D. Dai, J. Yang, Y.-C. Zou, J.-R. Wu, L.-L. Tan, Y. Wang, B. Li, T. Lu, B. Wang and Y.-W. Yang, Macrocyclic Arenes-Based Conjugated Macrocycle Polymers for Highly Selective CO_2 Capture and Iodine Adsorption, *Angew. Chem., Int. Ed.*, 2021, **60**, 8967–8975.
38 J. Cao, H. Zhu, L. Shangguan, Y. Liu, P. Liu, Q. Li, Y. Wua and F. Huang, A pillar[5]arene-based 3D polymer network for efficient iodine capture in aqueous solution, *Polym. Chem.*, 2021, **12**, 3517.
39 W.-Y. Pei, J. Yang, H. Wu, W. Zhou, Y.-W. Yang and J.-F. Ma, A calix[4]resorcinarene-based giant coordination cage: controlled assembly and iodine uptake, *Chem. Commun.*, 2020, **56**, 2491–2494.
40 T. Shan, L. Chen, D. Xiao, X. Xiao, J. Wang, X. Chen, Q.-H. Guo, G. Li, J. F. Stoddart and F. Huang, Adaptisorption of Nonporous Polymer Crystals, *Angew. Chem., Int. Ed.*, 2024, **63**, e202317947.
41 K. Jie, Y. Zhou, E. Li, Z. Li, R. Zhao and F. Huang, Reversible Iodine Capture by Nonporous Pillar[6]arene Crystals, *J. Am. Chem. Soc.*, 2017, **139**, 15320–15323.

42 Y. He, J. Wang, I. S. Sirotin, V. V. Kireev and J. Mu, Crosslinked Fluorinated Poly(arylene ether)s with POSS: Synthesis and Conversion to High-Performance Polymers, *Polymers*, 2021, **13**, 3489.

43 X. Ji, H. Wang, H. Wang, T. Zhao, Z. A. Page, N. M. Khashab and J. L. Sessler, Removal of Organic Micropollutants from Water by Macrocycle-Containing Covalent Polymer Networks, *Angew. Chem., Int. Ed.*, 2020, **59**, 23402–23412.